Journal of Applied Polymer Science

A facile synthesis of a novel three-phase nanocomposite: Single-wall carbon nanotube/silver nanohybrid fibers embedded in sulfonated polyaniline

Rajesh K. Agrawalla,[1,2] Subhasish Paul,[2] Pratap K. Sahoo,[3] Amit K. Chakraborty,[2] Apurba K. Mitra[1]*

[1]Nanoscience Laboratory, Department of Physics, National Institute of Technology Durgapur, Durgapur 713209, West Bengal, India

[2]Carbon Nanotechnology Laboratory, Department of Physics, National Institute of Technology Durgapur, Durgapur 713209, West Bengal, India

[3]Department of Physics, School of Physical Sciences, National Institute of Science Education and Research, Bhubaneswar 751005, Odisha, India

*Present address: Visiting Faculty, National Institute of Technology Durgapur, Durgapur 713209, WestBengal, India.
Correspondence to: A. K. Mitra (E-mail: akmrecdgp@yahoo.com)

ABSTRACT: A three-phase water-soluble nanocomposite of single wall carbon nanotube/silver nanoparticle hybrid fibers embedded in sulfonated polyaniline has been synthesized by a simple chemical solution mixing process. The nanocomposite has been characterized by high resolution electron microscopy, X-ray diffractometry, FTIR spectroscopy, Raman spectroscopy, and thermogravimetric analysis. Optical and electrical characteristics of the nanocomposite have been determined by UV–vis absorption spectroscopy, photoluminescence spectroscopy, and four-probe electrical conductivity measurement. A surface plasmon absorption band obtained around 460 nm indicates the presence of silver nanoparticles in the composite. The optical band gap calculation for sulfonated polyaniline vis-a-vis the nanocomposite supported the conductivity measurement. Over 1300 times increase in DC electrical conductivity has been observed for the three-phase nanocomposite, with a filler loading of 20 wt %, at 306 K. This observation could be explained by Mott's variable range hopping model considering a three-dimensional conduction. Such a nanocomposite has immense potential for use as a cathode material in lithium-ion batteries and supercapacitors. © 2014 Wiley Periodicals, Inc. J. Appl. Polym. Sci. **2015**, *132*, 41692.

KEYWORDS: batteries and fuel cells; composites; graphene and fullerenes; nanotubes; non-polymeric materials and composites; optical properties

Received 25 May 2014; accepted 28 October 2014
DOI: 10.1002/app.41692

INTRODUCTION

Polyaniline (PANI) is the most studied conducting polymer in recent years due to its numerous potential applications.[1–4] Carbon nanotubes (CNTs) possess excellent physical properties[5,6] and have been extensively used as reinforcing fibers in PANI matrix to improve the characteristic optical and electrical properties of the polymer.[7–12] Meng *et al.* succeeded in making paper-like CNT/PANI composite electrodes for energy storage devices and studied their electrochemical properties.[13] However, a major drawback of PANI is its insolubility in water. Water solubility is essential for many electrical applications. Sulfonation is one of the common methods to improve the solubility and processability of PANI in water. In this process, the emeraldine salt form of PANI is treated with chlorosulfonic acid in an inert solvent. The prepared sulfonated-PANI (SPANI) becomes water-soluble at all pH values. However, the presence of the strong electron-withdrawing sulfonic acid (—SO_3H) groups significantly reduces the conductivity of SPANI compared to that of pure PANI, limiting its electrical applications. Therefore, an improvement in the electrical conductivity of the water-soluble SPANI is very much required. Researchers have successfully combined CNTs with SPANI to form composites in which the idea was to exploit the excellent electrical properties of CNTs to increase the conductivity of the water-soluble nanocomposite. Zhao *et al.* synthesized a water-soluble SWCNT/poly(*m*-aminobenzene sulfonic acid—PABS) binary composite and observed much improved electrical conductivity.[14]

The PANI/CNT composites find application in biosensors,[10] supercapacitors,[15] metal-semiconductor devices,[16] and actuators.[17] Researchers have also tried to combine noble metal

nanoparticles with PANI as well as with PANI/CNT composite. Silver (Ag) nanoparticles have been combined with PANI and as a result the optical and electrical properties of the polymer have been found to improve significantly. An enhancement in the photoluminescence and electrical conductivity has been observed for PANI/Ag nanocomposite.[18] Gao *et al.*[19] synthesized PANI/Ag composite in the form of nanotubes and showed that its electrocatalytic activity toward reduction of dopamine was much better than pure PANI. Ag nanoparticles have been attached on the CNT surfaces to obtain a new category of hybrid materials which possess the combined properties of Ag nanoparticles and the CNTs. Such nanohybrids have numerous potential applications as catalyst,[20] optical limiter,[21] and so forth. Paul *et al.*[22] synthesized single-wall carbon nanotube/silver (SWCNT/Ag) nanohybrid and studied its optical and electrical properties. The PANI/CNT/Ag three-phase nanocomposite consists of three constituents namely, PANI, CNT, and Ag nanoparticle. This nanocomposite has achieved significant attention as it combines together the electrical properties of CNTs and the optical/catalytic properties of Ag nanoparticles. Such nanocomposites have been synthesized and their electrochemical behavior investigated by some researchers.[23,24] The investigations explored their suitability to be used as cathode materials in batteries and supercapacitors.

The purpose to synthesize ternary composites is to combine the interesting properties of each of the constituents. SPANI is relatively poor conductor of electricity but is known to have good specific capacitance, it is lightweight, and allows for flexible films. SWCNTs are known to be good conductor of electricity and heat, large surface area, and silver nanoparticles are excellent conductors of electricity apart from having good optical properties. Hence, the rationale for our work is to synthesize a novel composite with many interesting properties through the synergy of the properties of its constituents. This information has now been included in Introduction section.

In this work, PANI was synthesized and functionalized with sulfonate group to obtain SPANI. SWCNTs were purified and functionalized with carboxyl group by acid treatment. Silver nanoparticles were deposited on nanotube surfaces following a wet chemical process to obtain SWCNT/Ag hybrid nanostructures. A three-phase nanocomposite of SPANI embedded with SWCNT/Ag nanohybrid fibers was then synthesized by a simple chemical process. We adopted a solution mixing method to synthesize the nanocomposite as it has been a proven better method towards improving the electrical properties of the synthesized nanocomposites, and this fact has been established in the cases of other polymers such as polypropylene and polystyrene.[25] Thus, we could synthesize a water soluble nanocomposite, which has not been reported earlier, to the best of our knowledge. The increase in conductivity by over 1300 times is another significant achievement of this investigation.

EXPERIMENTAL

Materials

The SWCNTs used in our work were supplied by Chengdu Organic Chemicals, China. These were prepared by electric arc discharge method. The average diameter, length, and purity of the SWCNTs, as stated by the manufacturer were 1–2 nm, 1–3 μm, and 95 wt %, respectively. Aniline, 1,2-dichloroethane (DCE), and ammonium persulfate were supplied by Merck Specialties, Mumbai. The chlorosulfonic acid used in our work was supplied by LOBA Chemie, Mumbai. Except SWCNTs, all other chemicals were used as received without further purification.

Purification and Functionalization of SWCNTs

The as-received SWCNTs were purified by heating in a muffle furnace at 350°C in air for 1 h followed by soaking and stirring in 6*M* HCl for 12 h. The acid-treated SWCNTs were filtered using vacuum filtration system (Millipore, pore size ~0.22 μm) and washed thoroughly with deionized water. The purified SWCNTs were further treated in a mixture of concentrated HNO_3/H_2SO_4 in 1 : 3 volume proportion for 4 h followed by washing with dilute NaOH aqueous solution and filtration with Millipore filtration apparatus until the pH became neutral, thereby attaching carboxylic acid (—COOH) groups to obtain the functionalized single-walled carbon nanotubes (f-SWCNTs).

Synthesis of SWCNT/Ag Hybrid Nanostructure

For the preparation of SWCNT/Ag hybrid nanostructure, dimethyl sulfoxide (DMSO) was used as reducing agent and trisodium citrate dehydrate as capping agent to control the size of the nanoparticles. We added 0.2368 g of acid-treated SWCNT to 20 ml of DMSO. Simultaneously, 0.4 g of $AgNO_3$ was added to 20 ml of DMSO and stirred at 60°C using a magnetic stirrer (REMI 2MLH) followed by addition of 0.75 g of trisodium citrate. Both the solutions were mixed and stirred for 1 h. The resultant solution was then filtered using Whatman filter paper. The precipitate was washed thoroughly with deionized water followed by drying at 80°C in a Muffle furnace (Metrex Scientific Instruments, India) for 24 h to obtain SWCNT/Ag nanohybrid sample. The sample was then dried under IR lamp.

Synthesis of SPANI

0.2*M* aniline hydrochloride and 0.25*M* ammonium persulfate solutions were prepared and mixed in equal volumes and left overnight for polymerization to take place. The salt precipitate (PANI) was collected by filtration using a Whatman filter paper. It was then mixed with 1,2-DCE and heated to 80°C under stirring using a magnetic stirrer (REMI 2 MLH). Chlorosulfonic acid diluted with DCE was added drop-wise to the reaction mixture and stirred at 80°C for 1 h. A semi-solid precipitate, that is, sulfonated polyaniline (SPANI) obtained by filtration was then mixed with 400 ml water and heated to 60°C and stirred for 2 h to promote hydrolysis. The solution was further diluted with water and filtered through a cellulose membrane using a vacuum filtration system (Millipore). The final sample (SPANI) was collected over the filter membrane and dried in air at room temperature.

Synthesis of SPANI/SWCNT and SPANI/SWCNT/Ag Nanocomposites

Aqueous dispersion of f-SWCNTs was prepared by adding 0.03 g of f-SWCNTs in 20 ml of deionized water followed by sonication in an ultrasonic bath (250 W Piezo-Usonic). This dispersion was mixed with SPANI aqueous solution followed by stirring at 60°C for 3 h. The resulting solution was cooled and filtered using vacuum filtration apparatus (Millipore). The

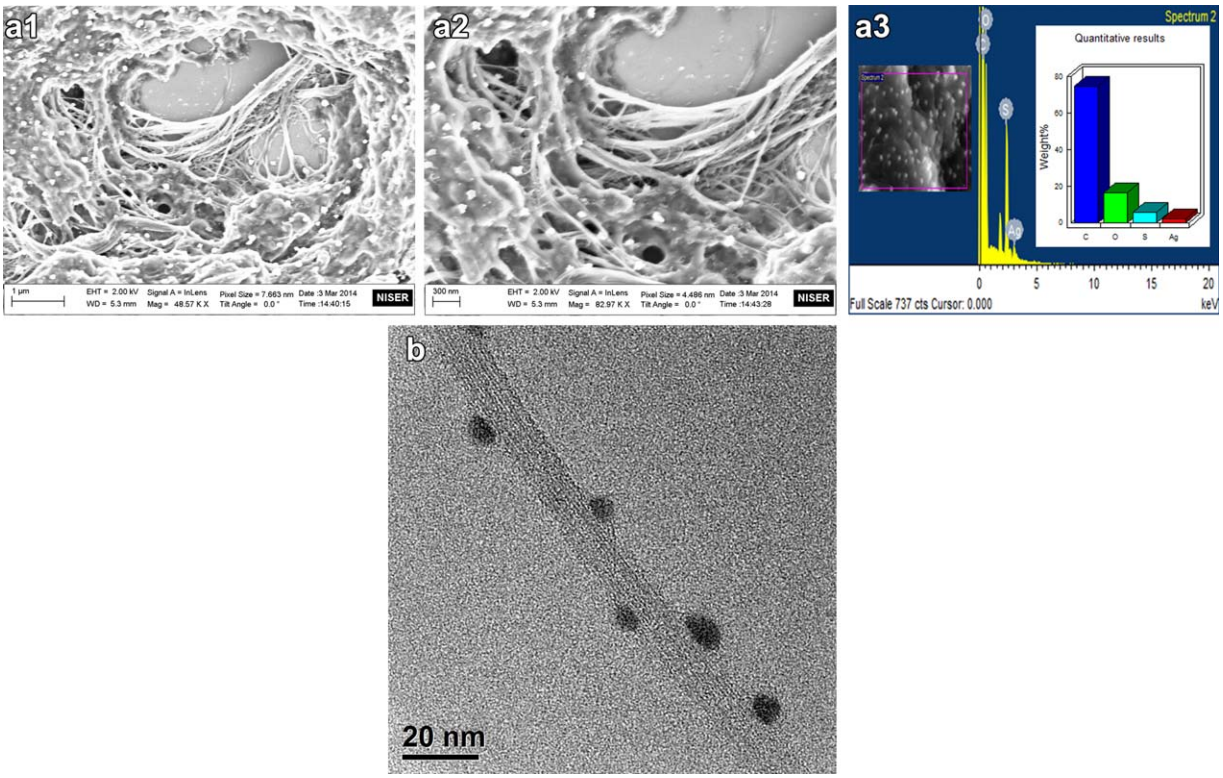

Figure 1. (a)1 FESEM image of SPANI/f-SWCNT/Ag composite; (a) 2 FESEM image of SPANI/f-SWCNT/Ag composite at higher resolution; (a) 3 FESEM image of SPANI/f-SWCNT/Ag composite with EDAX analysis. (b) HRTEM micrograph of a f-SWCNT bundle with Ag nanoparticles attached on surface and embedded in SPANI matrix. [Color figure can be viewed in the online issue, which is available at wileyonlinelibrary.com.]

sample collected by filtration was dried in air at room temperature to get SPANI/SWCNT composite with 6 wt % of f-SWCNTs. The whole process of solution mixing was repeated for SWCNT/Ag nanohybrids to obtain SPANI/SWCNT/Ag nanocomposite. We have added 0.09 g of SWCNT/Ag nanohybrid fillers into deionized water followed by mixing with SPANI solution to obtain the desired composite. The SPANI/SWCNT/Ag nanocomposite contained 8 wt % of f-SWCNT/Ag nanohybrid fillers. The weight percentage of SWCNTs and SWCNT/Ag hybrid fibers in the respective composites was estimated by weighing the composite powder samples obtained after drying.

Characterization of the Samples

The micrographs of the samples were obtained using high resolution transmission electron microscope (HRTEM model JEOL JEM-2010; operating acceleration voltage 200 kV). The XRD patterns were obtained using Philips PANalytical X-Pert Pro diffractometer. The molecular structures of the samples were characterized by a Perkin Elmer Spectrum RX-I FTIR Spectrometer. The laser source used in the spectrometer was a He–Ne laser (633 nm). Raman spectroscopy was performed using EZ Raman—M field portable Raman analyzer (Enwave Optronics). A diode laser of wavelength 785 nm was used as excitation source. The thermogravimetric analysis (TGA) was performed with PerkinElmer Pyris-1 TGA at the heating rate of 10°C/min in nitrogen atmosphere. The optical absorbance spectra were recorded using a HITACHI U-3010 UV–visible absorption spectrophotometer. Photoluminescence spectra of the samples were acquired using a PerkinElmer LS-55 fluorescence spectrophotometer. The electrical conductivity of the samples was measured by a Four-Probe set-up (DFP-02, Scientific Equipment).

Table I. Elemental Analysis of the SPANI/f-SWCNT/Ag Nanocomposite with 6 wt % Loading of the f-SWCNT/Ag Nanohybrid in SPANI

Element	Peak area	Area sigma	*k* factor	Abs corrn.	Weight %	Weight % sigma	Atomic %
C K	1389	72	2.208	1.000	71.44	3.16	83.47
N K	147	50	2.965	1.000	10.13	3.14	10.15
O K	89	36	1.810	1.000	3.74	1.47	3.28
S K	177	26	0.940	1.000	3.88	0.60	1.70
Ag L	269	41	1.724	1.000	10.82	1.58	1.41
Totals					100.00		

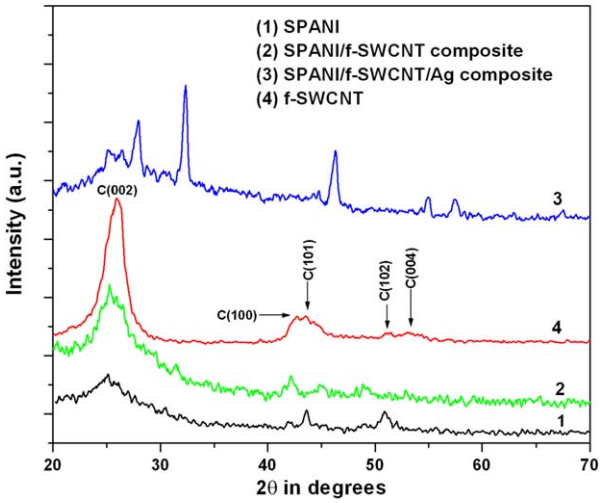

Figure 2. XRD pattern of SPANI, f-SWCNT, SPANI/f-SWCNT, and SPANI/f-SWCNT/Ag. [Color figure can be viewed in the online issue, which is available at wileyonlinelibrary.com.]

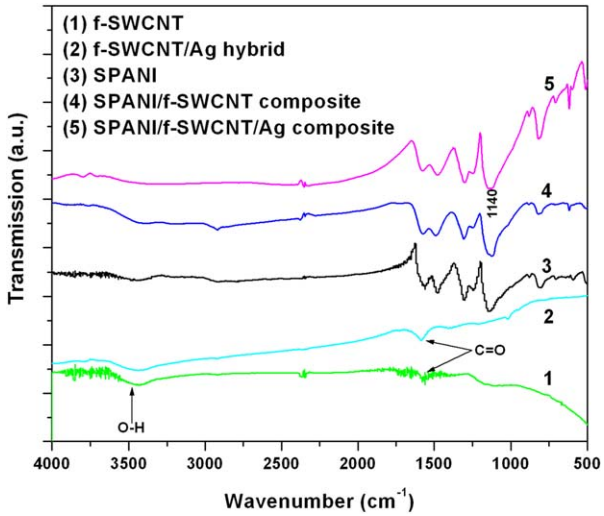

Figure 4. FTIR spectra of SWCNT, f-SWCNT/Ag, SPANI, SPANI/f-SWCNT, and SPANI/f-SWCNT/Ag. [Color figure can be viewed in the online issue, which is available at wileyonlinelibrary.com.]

For conductivity measurement by Four-Probe method, the composite powder samples were compressed into disc pellets having diameter of 1.25 cm and a thickness of 2.0 mm, using hydraulic press at a pressure of 2.5 tonnes/inch.

RESULTS AND DISCUSSION

The FESEM images of SPANI/f-SWCNT/Ag nanocomposite are shown in Figure 1(a1,a2). The Figure 1(a3) shows the EDAX spectrum. Table I gives the elemental analysis of the nanocomposite. In Figure 1(b), the HRTEM micrograph of the sample is shown. The different components of the ternary composite, such as SPANI, f-SWCNTs, and silver nanoparticles, are clearly distinguishable in the micrographs. The dark particles (in the HRTEM micrograph) represent the silver nanoparticles which are nearly spherically shaped having diameter in the range 5–15 nm. They are almost uniformly attached to the surfaces of f-SWCNTs to form f-SWCNT/Ag hybrid nanostructures, which are embedded in the matrix of SPANI. The EDAX spectrum of the sample confirms the presence of silver (Ag) and carbon (C) in the sample. Carbon is obtained both from SPANI and f-SWCNT. The presence of copper (Cu) is due to the use of copper grid over which the sample was mounted.

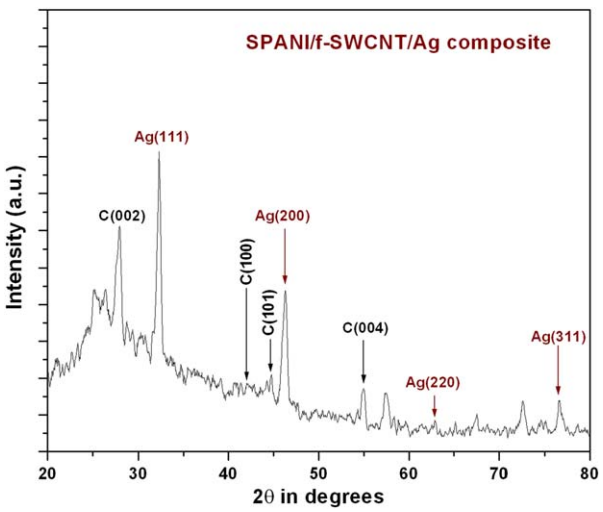

Figure 3. Labeled XRD pattern of SPANI/f-SWCNT/Ag nanocomposite. [Color figure can be viewed in the online issue, which is available at wileyonlinelibrary.com.]

The structural characteristics of SPANI, f-SWCNT, SPANI/f-SWCNT binary composite, and SPANI/f-SWCNT/Ag ternary composite (6 wt % loading) have been analyzed from X-ray diffractograms shown in Figures 2 and 3. In the XRD pattern of SPANI, there are three prominent humps at about $2\theta = 25°$, 43.5°, and 51°.[26,27] No crystalline peak of SPANI was observed as SPANI is amorphous. In f-SWCNT, the peaks are at 26°, 42.5°, 44°, 51°, and 53.5° and these correspond to (002), (100), (101), (102), and (004) reflections, respectively, of the graphitic planes of the nanotubes (JCPDS card no. 75–1621). The pattern of SPANI/f-SWCNT composite shows no new peak, which implies that no additional order has been introduced. In the diffractogram of SPANI/f-SWCNT/Ag ternary composite, apart from the humps assigned to SPANI and peaks assigned to f-SWCNT, we also observe sharp peaks assigned to (111), (200), (220), and (311) planes of the cubic phase of Ag in its face centered crystal structure (JCPDS card no. 04-0783). This also agrees well with earlier report.[23] The average size of Ag nanoparticles of the composite system was estimated to be 15 nm using the Debye–Scherrer formula.[28]

In FTIR spectra, the stretches at different points indicate the absorption bands, shown in Figure 4. The stretch near 3450 cm^{-1}, for all samples, indicates the stretching vibration arising from the absorption of water by KBr used for analysis. The spectrum of f-SWCNT has stretches near 1600 cm^{-1} due to C═O vibration formed due to acid treatment. The spectrum of f-SWCNT/Ag hybrid matches with that of f-SWCNT. SPANI shows the characteristic stretches at 1560, 1480, 1300, and 1140 cm^{-1}. The stretches at 1560 and 1480 cm^{-1} arise due to the stretching vibrations of quinoid ring (—N═quinoid═N—)

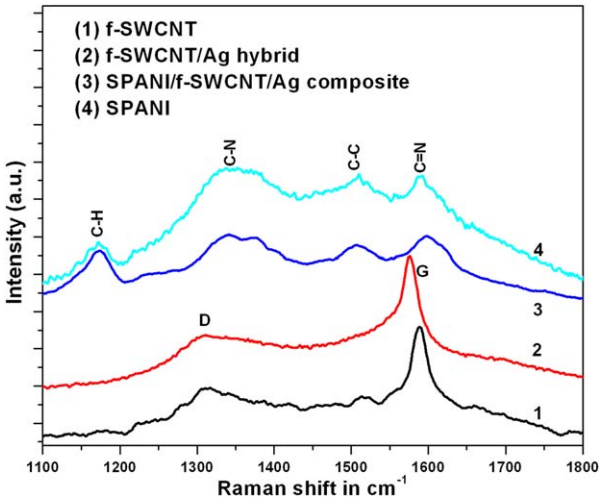

Figure 5. Raman spectra of SPANI, f-SWCNT, f-SWCNT/Ag, and SPANI/f-SWCNT/Ag. [Color figure can be viewed in the online issue, which is available at wileyonlinelibrary.com.]

and the benzenoid ring (—N—benzenoid—N—), respectively. The stretches at 1300 and 1140 cm^{-1} are due to C—N stretching and C═N stretching, respectively. The prominent stretch at 1140 cm^{-1} represents the characteristic stretch of conductivity of SPANI and it measures the degree of delocalization of electrons. The FTIR spectra of SPANI/f-SWCNT and SPANI/f-SWCNT/Ag composites perfectly match with that of SPANI, which indicates good coating of nanotubes and hybrids with SPANI. The FTIR spectrum confirms that the f-SWCNT/Ag hybrids were embedded in the polymer matrix. We also observe increase in the intensity of the characteristic conductivity stretch at 1140 cm^{-1} of the polymer for the SPANI/f-SWCNT/Ag composite. This is also supported by enhanced electrical conductivity of the ternary composite.

The Figure 5 shows the Raman spectra of SPANI, f-SWCNT, f-SWCNT/Ag nanohybrid, and SPANI/f-SWCNT/Ag nanocomposite. In the Raman spectrum of SPANI, the peak at 1596 cm^{-1} arises from C—C stretching of the benzenoid ring and the peak at 1504 cm^{-1} comes from C═N stretching of the quinonoid ring. The peak at 1339 cm^{-1} arises from the C—N^+ stretching and that of 1174 cm^{-1} arises from C—H bending of the quinoid/benzenoid ring. The Raman spectrum of SWCNTs shows the normal characteristic peaks, the G-band at 1589 cm^{-1} and the D-band at 1314 cm^{-1}. The G-band originates from in-plane vibrations of the graphitic wall and the D-band originates from defects in the graphitic structure. The position of G-band of pristine SWCNT is red-shifted from 1589 to 1575 cm^{-1} on decorating with Ag nanoparticles, which indicates charge transfer and electronic interaction between Ag nanoparticles and SWCNT bundles. Similar down-shift has also been observed earlier by several researchers.[22,29,30] Further, the I_D/I_G factor is increased on decorating f-SWCNTs with Ag nanoparticles. For pristine f-SWCNTs, the ratio of the intensity of D-band and that of G-band, that is, I_D/I_G is 0.512, while for f-SWCNT/Ag hybrid, it has been found to be 0.555. This increase in I_D/I_G factor indicates that the Ag nanoparticles are attached to the SWCNT surfaces.[21] In the Raman spectrum of the ternary composite, the effect of the polymer is dominant with a significant increase in the ratio of intensity of C—N^+ stretching and C—H bending vibrations (I_{C-N+}/I_{C-H}). It indicates that a good coating of the SWCNT/Ag nanohybrids with SPANI has been achieved. These results of the Raman spectra are supported by the HRTEM images, where we observe attachment of Ag nanoparticles to the surface as well as the coating of the hybrid by the polymer.

Figure 6 shows the TGA thermograms of f-SWCNT, SPANI, and SPANI/f-SWCNT/Ag composite. The f-SWCNT has a higher thermal stability than other samples and it shows no appreciable weight loss up to about 500°C. The three-step decomposition process of SPANI has already been explained in Chapter-4. The thermogram of SPANI/f-SWCNT/Ag composite almost matches with that of SPANI, which may be due to very low content of reinforcement of nanohybrid. We observe almost total weight loss of SPANI and f-SWCNT. But for SPANI/f-SWCNT/Ag nanocomposite, some residual weight (of about 3%) is observed in the sample in the temperature range of 600–700°C. This is due to the undecomposed silver content present in the nanocomposite. The TGA analysis indicates higher thermal stability for SPANI/f-SWCNT/Ag composite than SPANI.[23,24]

The UV–visible absorption spectra of SPANI, SPANI/f-SWCNT, and SPANI/f-SWCNT/Ag are compared in Figure 7. The spectrum of SPANI consists of humps at 355 nm (π–π^* transition), 455 nm (polaron-π^* transition), and beyond 750 nm (π-polaron transition). The shift of the first and second absorbance bands in the SPANI/f-SWCNT binary composite has been explained in Chapter-4. In SPANI/f-SWCNT/Ag ternary composite, the features of SPANI/f-SWCNT composite have been modified due to the surface plasmon resonance (SPR) band of Ag nanoparticles. The absorption band around 365 nm may be assigned to the SPR band of Ag nanoparticles. Earlier, SPR band for Ag nanoparticles in PANI/Ag binary composite has been obtained at 380 nm.[18]

The optical band gaps of the investigated samples were estimated (Figure 8) using Tauc relation. The optical band gaps of

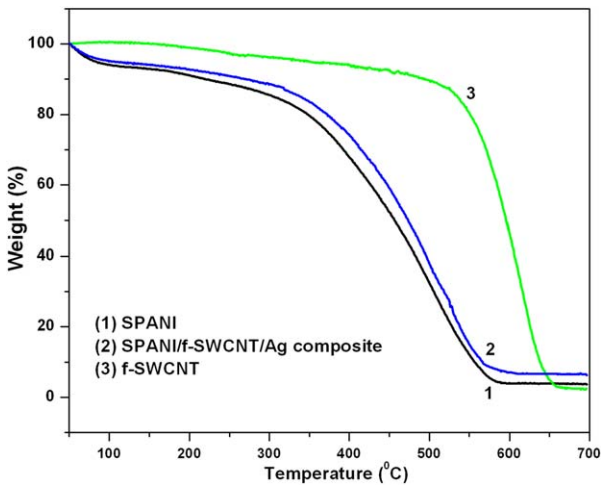

Figure 6. Thermograms of SPANI, f-SWCNT, and SPANI/SWCNT/Ag composite. [Color figure can be viewed in the online issue, which is available at wileyonlinelibrary.com.]

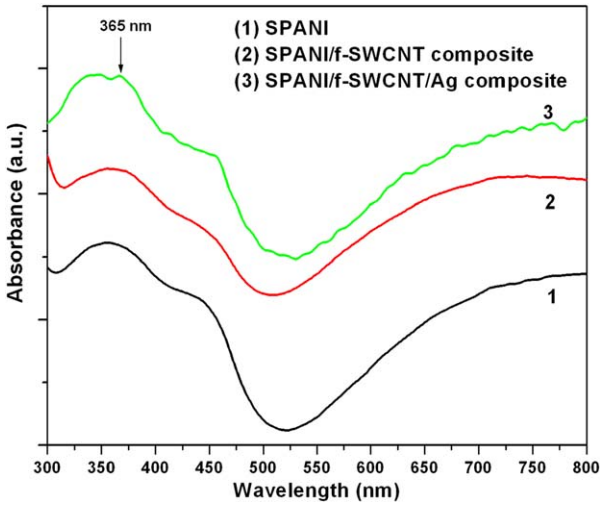

Figure 7. UV–vis absorbance spectra of SPANI, SPANI/f-SWCNT, and SPANI/f-SWCNT/Ag. [Color figure can be viewed in the online issue, which is available at wileyonlinelibrary.com.]

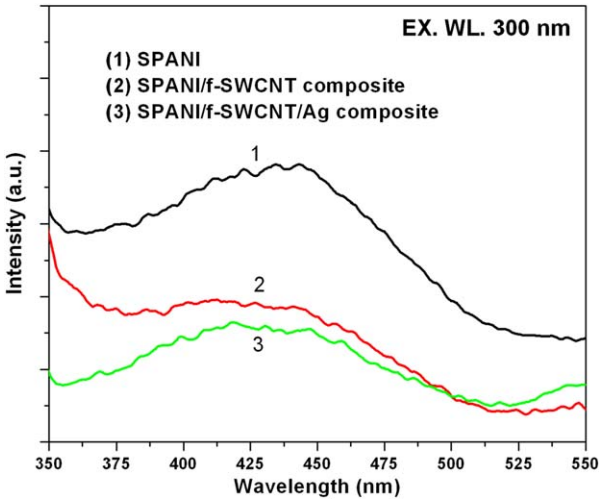

Figure 9. Photoluminescence spectra for SPANI, SPANI/f-SWCNT, and SPANI/f-SWCNT/Ag at 300 nm excitation wavelength. [Color figure can be viewed in the online issue, which is available at wileyonlinelibrary.com.]

SPANI, SPANI/f-SWCNT binary composite, and SPANI/f-SWCNT/Ag ternary composite were estimated to be 3.75, 3.66, and 3.55 eV, respectively. The decrease in the band gap is compatible with the increase in conductivity. We observe that the decrease in the band gap is more when the polymer is reinforced with f-SWCNT/Ag nanohybrids rather than with pristine f-SWCNTs. Decrease in band gap of PANI on reinforcing silver nanoparticles into its matrix has been reported earlier.[18]

Photoluminescence spectra for SPANI and the two composites such as SPANI/f-SWCNT and SPANI/f-SWCNT/Ag are obtained for an excitation wavelength of 300 nm and are shown in Figure 9. SPANI shows a hump around 445 nm. There is a quenching effect of the broad emission band of SPANI upon interactions with SWCNTs. The fluorescence is also diminished when nanotubes hybridized with silver nanoparticles are embedded into the polymer matrix. The quenching generally takes place when the polymer is doped to a highly conductive state.[31] The quenching takes place as a result of energy transfer between SPANI and the hybrid. Figure 10 shows the emission spectra of SPANI/f-SWCNT/Ag composite for a range of excitation wavelengths from 260 to 300 nm. We observe quenching effect in the emission band as well as a red shift with increasing excitation wavelength. This indicates that the number of energetic electrons taking part in the transition process decreases with increase in excitation wavelength.

The Figure 11 shows the DC electrical conductivity of SPANI, SPANI/f-SWCNT, and SPANI/f-SWCNT/Ag composites at temperatures ranging from 318 to 353 K. We observe an increase in the conductivity with increasing temperature for all the samples, thus showing semiconductor like behavior. On adding

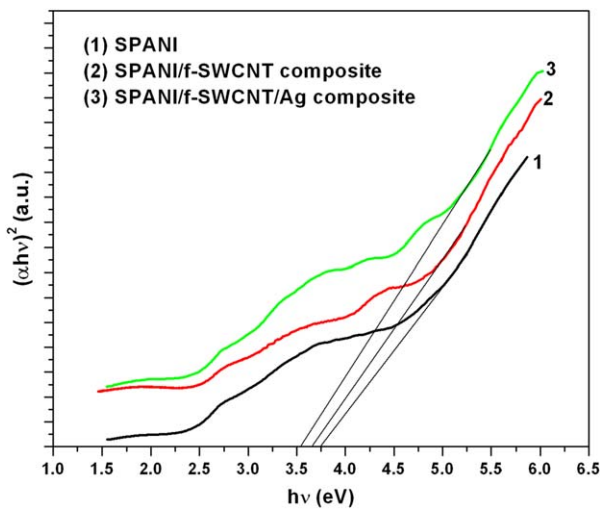

Figure 8. Plot of $(\alpha h\nu)^2$ versus $h\nu$ for SPANI, SPANI/f-SWCNT, and SPANI/f-SWCNT/Ag. [Color figure can be viewed in the online issue, which is available at wileyonlinelibrary.com.]

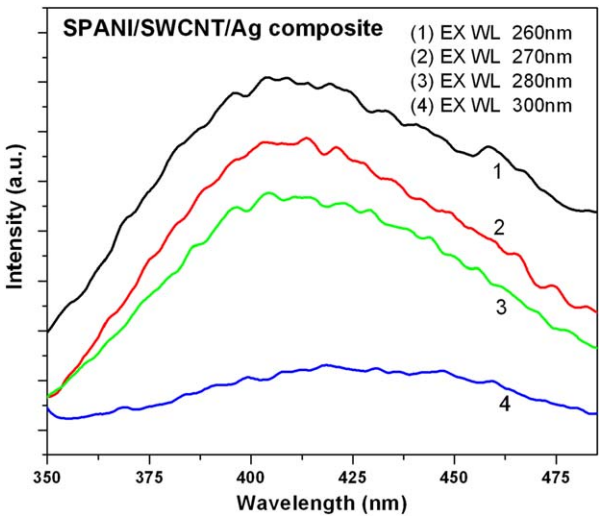

Figure 10. Photoluminescence spectra for SPANI/SWCNT/Ag composite at various excitation wavelengths. [Color figure can be viewed in the online issue, which is available at wileyonlinelibrary.com.]

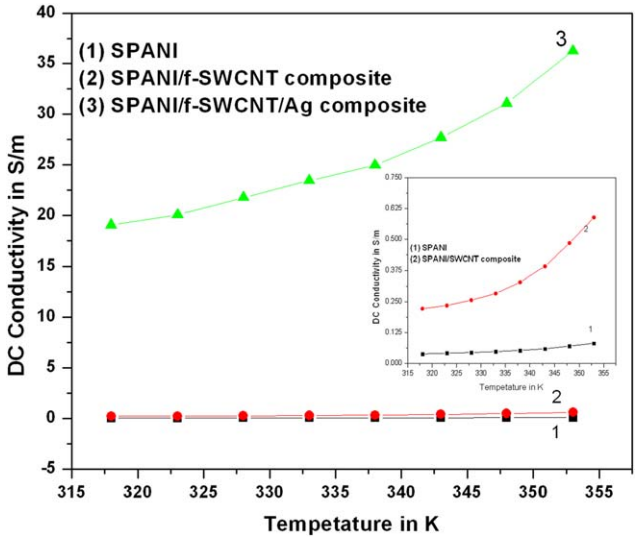

Figure 11. Comparison of conductivity of SPANI/f-SWCNT/Ag composite with SPANI and SPANI/f-SWCNT composite with varying temperature; comparison between SPANI and SPANI/f-SWCNT is shown in the inset. [Color figure can be viewed in the online issue, which is available at wileyonlinelibrary.com.]

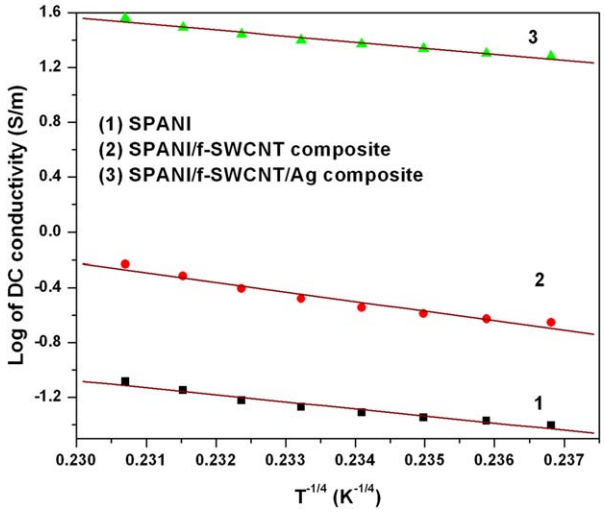

Figure 12. Variation of log of DC conductivity of SPANI, SPANI/f-SWCNT, and SPANI/f-SWCNT/Ag with $T^{-1/4}$ ($K^{-1/4}$) satisfying VRH model with $\gamma = 1/4$. [Color figure can be viewed in the online issue, which is available at wileyonlinelibrary.com.]

nanotubes or the nanohybrids to the polymer, the conductivity has increased. The value of conductivity for SPANI/f-SWCNT/Ag nanocomposite at 318 K is 480 times and 85 times higher than SPANI and SPANI/f-SWCNT composite, respectively. At 353 K, the conductivity of the ternary composite becomes 440 times and 61.5 times higher than that of SPANI and SPANI/f-SWCNT composite, respectively. The enhanced conductivity of the ternary composite is attributed to the presence of silver nanoparticles in it. Moreover, this enhancement is much larger than that of binary PANI/Ag composite reported earlier.[18] The conductivity measurement supports the optical band gap calculation.

The investigated samples behave as disordered semiconductors[32] and Mott's variable range hopping (VRH) model is suitable for explaining the temperature dependence of conductivity for such systems.[33] We find that the log of DC conductivity of all samples show linear variation with $T^{-1/4}$, and therefore satisfy three-dimensional (3D) VRH transport mechanism (Figure 12). Such 3D charge transport mechanism in conducting PANI and PANI/CNT composites has been reported earlier.[34] We obtained the values of T_0 for the three samples from the slopes of the linear variation of log σ with $T^{-1/4}$. The estimated values of T_0 were 4,380,910, 13,845,841, and 2,825,761 K for SPANI, SPANI/f-SWCNT binary, and SPANI/f-SWCNT/Ag ternary composite, respectively. Mott temperature has increased for the binary composite and it has decreased for the ternary composite. We see that T_0 for SPANI/f-SWCNT/Ag is much lower than that for other samples owing to introduction of SWCNT/Ag nanohybrids into the matrix of SPANI.

Further to study the effect of the concentration of the reinforcing SWCNT/Ag hybrid fillers on the electrical conductivity of the nanocomposite, we synthesized more samples of the ternary composite having different f-SWCNT/Ag contents such as 5 wt %, 10 wt %, and 20 wt % and evaluated their electrical properties as follows.

At 306 K, the DC conductivity value of S1 (SPANI) is 0.034 S/m. It increases to 0.211 S/m (6.2 times) for S2 (SPANI/f-SWCNT binary composite with 10 wt % of SWCNT). For the ternary composites S3, S4, and S5, further increase in conductivity value takes place. The conductivity becomes 16.22 S/m (477 times), 26.01 S/m (765 times), and 44.99 S/m (1323 times); for samples S3, S4, and S5, respectively, compared to SPANI. Samples S3, S4, and S5 have 5 wt %, 10 wt %, and 20 wt % of hybrid content, respectively. Thus, with increase in SWCNT/Ag content in the three-phase nanocomposites from 0 to 20 wt %, we observed a sharp increase in the value of their electrical conductivity.

It is interesting to observe that the conductivity for SPANI/f-SWCNT/Ag ternary composite (with 5 wt % of f-SWCNT/Ag

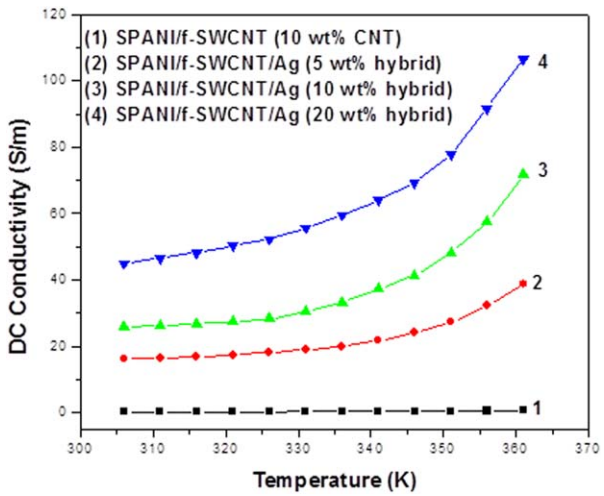

Figure 13. Comparison of conductivity of SPANI/f-SWCNT binary composite and SPANI/f-SWCNT/Ag ternary composites with varying temperature. [Color figure can be viewed in the online issue, which is available at wileyonlinelibrary.com.]

hybrid) is 77 times higher than that of SPANI/f-SWCNT binary composite (with 10 wt % of f-SWCNT). This indicates that silver plays a dominant role in the enhancement of the conductivity of the composites. The Figure 13 shows the variation of DC conductivity of the samples with temperature.

We observe that the electrical conductivity increases with temperature for all the samples; thus all the samples exhibit semiconducting behavior. As the filler content is doubled from 5 to 10 wt %, the electrical conductivity of the ternary nanocomposite increases to 1.60 times, whereas when the filler content increases to 20 wt %, the conductivity increases to 1.73 times of the sample with 10 wt % of the filler content. Thus, there is no sign of saturation of the conductivity value with increasing filler content.

CONCLUSIONS

In this study, we described the synthesis and characterization of a water-soluble ternary nanocomposite of SPANI embedded with f-SWCNT/Ag nanohybrid fillers. The sulfonation induces self-doping which allows conduction in SPANI in a larger pH range than in PANI, as observed by Bernard and Hugot-Le Goff.[35] Feng *et al.* synthesized a nanocomposite of sulfonated graphene with polyaniline.[36]

The attachment of silver nanoparticles to the surfaces of the nanotubes as well as the coating of the hybrid fibers by the polymer is evident from HRTEM images. The UV–visible absorption spectrum of the nanocomposite showed the modified surface plasmon resonance band associated with silver nanoparticles. The optical band gap calculation of SPANI vis-a-vis the nanocomposite supported the electrical conductivity measurement. The ternary nanocomposite showed excellent electrical conductivity when compared with both SPANI and SPANI/f-SWCNT binary composite. A 1323 times increase in DC conductivity has been observed for the ternary composite with 20 wt % of filler loading, when compared with the value for the polymer at 306 K. A three-dimensional VRH conduction mechanism has been satisfied by the ternary composite. Ge *et al.* proposed a method to prepare transparent and flexible supercapacitors assembled from PANI/SWCNT composite thin film electrodes.[37] Recently flexible microelectronic circuits were fabricated via the screen-printing technique using ternary composites of PANI/Ag/MWCNTs by Li *et al.*[38]

Here, we present a simple chemical synthesis of a novel polymeric material which may have greater potential for application as cathode material in lithium ion batteries and supercapacitors.

REFERENCES

1. Bhadra, S.; Khastgir, D.; Singha, N. K.; Lee, J. H. *Prog. Polym. Sci.* **2009**, *34*, 783.
2. Arslan, A.; Hur, E. *Int. J. Electrochem. Sci.* **2012**, *7*, 12558.
3. Dhand, C.; Das, M.; Datta, M.; Malhotra, B. D. *Biosens. Bioelectron.* **2011**, *26*, 2811.
4. Gao, J.; Sansinena, J. M.; Wang, H. L. *Chem. Mater.* **2003**, *15*, 2411.
5. Iijima, S. *Nature* **1991**, *354*, 56.
6. Dresselhaus, M. S.; Dai, H. J. *MRS Bull.* **2004**, *29*, 237.
7. Kar, P.; Choudhury, A. *Sens. Actuators B* **2013**, *183*, 25.
8. Lafuente, E.; Callejas, M. A.; Sainz, R.; Benito, A. M.; Maser, W. K.; Sanjuan, M. L.; Saurel, D; Teresa, J. M.; Martinez, M. T. *Carbon* **2008**, *46*, 1909.
9. Kang, M. S.; Shin, M. K.; Ismail, Y. A.; Shin, S. R.; Kim, S. L.; Kim, H.; Lee, H.; Kim, S. *J. Nanotechnology* **2009**, *20*, 085701.
10. Dhand, C.; Solanki, P. R.; Datta, M.; Malhotra, B. D. *Electroanalysis* **2010**, *22*, 2683.
11. Wu, T. M.; Lin, Y. W.; Liao, C. S. *Carbon* **2005**, *43*, 734.
12. Lin, Y. W.; Wu, T. M. *Compos. Sci. Technol.* **2009**, *69*, 2559.
13. Meng, C.; Liu, C.; Fan, S. *Electrochem. Commun.* **2009**, *11*, 186.
14. Zhao, B.; Hu, H.; Haddon, R. C. *Adv. Funct. Mater.* **2004**, *14*, 1.
15. Gupta, V.; Miura, N. *Electrochim. Acta* **2006**, *52*, 1721.
16. Ramamurthy, P. C.; Malshe, A. M.; Harrell, W. R.; Gregory, R. V.; McGuire, K.; Rao, A. M. *Solid State Electron.* **2004**, *48*, 2019.
17. Tahhan, M.; Truong, V. T.; Spinks, G. M.; Wallace, G. G. *Smart Mater. Struct.* **2003**, *12*, 626.
18. Gupta, K.; Jana, P. C.; Meikap, A. K. *Synth. Met.* **2010**, *160*, 1566.
19. Gao, Y.; Shan, D.; Cao, F.; Gong, J.; Li, X.; Ma, H.; Su, Z.; Qu, L. *J. Phys. Chem. C* **2009**, *113*, 15175.
20. Guo, D. J.; Li, H. L. *Carbon* **2005**, *43*, 1259.
21. Chin, K. C.; Gohel, A.; Chen, W. Z.; Elim, H. I.; Ji, W.; Chong, G. L.; Sow, C. H.; Wee, A. T. S. *Chem. Phys. Lett.* **2005**, *409*, 85.
22. Paul, R.; Maity, A.; Mitra, A.; Kumbhakar, P.; Mitra, A. K. *J. Nanopart. Res.* **2011**, *13*, 5749.
23. Kim, K.-S.; Park, S.-J. *J. Solid State Chem.* **2011**, *184*, 2724.
24. Nguyen, V. H.; Shim, J. J. *Synth. Met.* **2011**, *161*, 2078.
25. Xin, F.; Li, L. *Compos. Part A* **2011**, *42*, 961.
26. Karim, M. R.; Lee, C. Y.; Park, Y.-T.; Lee, M. S. *Synth. Met.* **2005**, *151*, 131.
27. Luzny, W.; Banka, E. *Macromolecules* **2000**, *33*, 425.
28. Klug, H. P.; Alexander, L. E. X-ray Diffraction Procedures for Polycrystalline and Amorphous Materials; Wiley: New York, **1954**.
29. Rao, A. M.; Eklund, P. C.; Bandow, S.; Thess, A.; Smalley, R. E. *Nature* **1997**, *388*, 257.
30. Samanasekera, G. U.; Allen, J. L.; Fang, S. L.; Loper, A. L.; Rao, A. M.; Eklund, P. C. *J. Phys. Chem. B* **1999**, *103*, 4292.
31. Shimano, J. Y.; MacDiarmid, A. G. *Synth. Met.* **2001**, *123*, 251.
32. Skotheim, T.; Elsebaumer, R. Handbook of Conducting Polymers; Marcel Dekker: New York, **1998**.
33. Mott, N. F.; Davis, E. Electronic Processes in Noncrystalline Materials; Oxford University Press: New York, **1979**.

34. Ghatak, S.; Chakraborty, G.; Meikap, A. K.; Woods, T.; Babu, R.; Blau, W. J. *J. Appl. Polym. Sci.* **2011**, *119*, 1016.

35. Bernard, M. C.; Hugot-Le Goff, A. *Electrochim. Acta* **2006**, *52*, 2.

36. Feng, W.; Zhang, Q.; Li, Y.; Feng, Y. *J. Solid State Electrochem.* **2013**, *18*, 4.

37. Jun Ge, J.; Cheng, G.; Chen, L. *Nanoscale* **2011**, *3*, 3084.

38. Li, J.; Liu, L.; Zhang, D.; Yang, D.; Guo, J.; Wei, J. *Synth. Met.* **2014**, *192*, 15.